An analytic model for high-contrast gratings

(Article begins on next page)

18 April 2024

An analytic model for high-contrast gratings

R. Orta,[1,2,]* A. Tibaldi,[2] P. Debernardi[2]

[1]*Department of Electronics and Telecommunications, Politecnico di Torino, Turin 10129, Italy*
[2]*Consiglio Nazionale delle Ricerche, Istituto di Elettronica e di Ingegneria dell'Informazione e delle Telecomunicazioni, Turin 10129, Italy*
*renato.orta@polito.it

Abstract: A new analytic model for high-contrast gratings is introduced, based on their description as bimodal Fabry-Pérot interferometers. It can be shown that their reflectivity and transmissivity can be decomposed into two interfering single-mode responses. A new parametrization of unitary symmetric matrices is introduced to describe the mirrors, opening up the possibility to obtain a fully analytic model. As an application example, the characterization of a high-contrast grating high-Q resonator is presented.

1 Introduction

High-contrast gratings (HCGs) are periodic arrays of dielectric bars with high refractive index, surrounded by a low-index medium [1]. Since these devices exhibit their extraordinary features when operating in the near-wavelength regime, where the bar region supports two propagating modes, their analysis has been always based on full-wave electromagnetic simulators such as the rigorous coupled wave analysis (RCWA) [2,3].

This work presents a new analytic framework describing the physics of HCGs viewed as bimodal Fabry-Pérot interferometers (FPIs) [4]. It is shown that the response of a bimodal FPI can be decomposed into the sum of two single-mode constituents. The key element of our approach is the parametrization of the mirror scattering matrices, which allows to obtain explicit expressions of the FPI response.

2. Parametrization of bimodal Fabry-Pérot interferometers

A bimodal FPI consists of two mirrors defining a cavity (inner region) where two modes are above cut-off, whereas in the outer halfspaces only one plane wave propagates. Hence, the mirrors, assumed to be identical, are characterized by 3x3 scattering matrices $\overline{S}$.

The device reflection and transmission responses are obtained by cascading the matrices of the two mirrors and of the bimodal cavity transmission lines. In the case of lossless mirrors, such responses exhibit exotic features, *e.g.* 100% reflection peaks or Fano resonances (quick zero-one transitions). In fact, the cascade involves the inversion of the matrix $(\mathbf{I} - \mathbf{T})$, where $\mathbf{I}$ is the identity and $\mathbf{T}$ is the generalized loop-gain matrix of the inner region, accounting for coupling between the cavity modes. By exploiting the eigen-decomposition of $\mathbf{T}$, the bimodal FPI responses can be decomposed into two single-mode constituents. Even if these contributions do not exhibit high-Q resonances or total reflection points taken singularly, their interference does.

These intuitions can be rigorously proved by the analytic formulas, which can be obtained by parameterizing the 3x3 mirror scattering matrices. This is obtained by enforcing unitarity and symmetry of each mirror scattering matrix, leading to the following expressions:

$$\overline{S}_{11} = \mathrm{e}^{-\mathrm{j}(\varphi_c + \Delta/2)} \left[\mathrm{e}^{\mathrm{j}\Psi} \cos^2 \Phi \cos \Theta - \mathrm{e}^{-\mathrm{j}\Psi} \sin^2 \Phi \right]$$

$$\overline{S}_{22} = \mathrm{e}^{-\mathrm{j}(\varphi_c - \Delta/2)} \left[\mathrm{e}^{-\mathrm{j}\Psi} \cos^2 \Phi - \mathrm{e}^{\mathrm{j}\Psi} \sin^2 \Phi \cos \Theta \right]$$

$$\overline{S}_{12} = \frac{1}{2}\mathrm{j}\mathrm{e}^{-\mathrm{j}\varphi_c} \sin 2\Phi \left[\mathrm{e}^{-\mathrm{j}\Psi} + \mathrm{e}^{\mathrm{j}\Psi} \cos \Theta \right]$$

$$\overline{S}_{13} = \mathrm{j}\mathrm{e}^{\mathrm{j}\frac{-\varphi_c + \varphi_{33} + \Psi}{2}} \mathrm{e}^{-\mathrm{j}\frac{\Delta}{4}} \sin \Theta \cos \Phi$$

$$\overline{S}_{23} = -\mathrm{e}^{\mathrm{j}\frac{-\varphi_c + \varphi_{33} + \Psi}{2}} \mathrm{e}^{\mathrm{j}\frac{\Delta}{4}} \sin \Theta \sin \Phi$$

$$\overline{S}_{33} = \mathrm{e}^{\mathrm{j}\varphi_{33}} \cos \Theta.$$

Here, the indexes {1,2} and 3 refer to the inner and to the outer ports, respectively. So, six real parameters ($\Theta, \Phi, \Psi, \Delta, \varphi_c, \varphi_{33}$) characterize completely the junction scattering matrix, which in general consists of nine complex numbers. It can be noted that the magnitude of the scattering parameters for outer incidence describes the surface of a unit sphere by changing the parameters Θ and Φ, which can be then interpreted as zenith and azimuth angles, as shown in Fig. 1.

This parametrization can be exploited to write analytic expressions of the bimodal FPI interferometer response. As an example, Fig. 2 shows reflectivity and transmissivity for the parameters of Fig. 1 versus the average of the cavity electrical lengths, $\overline{\theta}$. This shows the capability of the model to describe the aforementioned features. On the other hand, these responses clearly resemble those of a single-mode FPI plus the Fano resonance, as suggested from the loop gain eigen-decomposition.
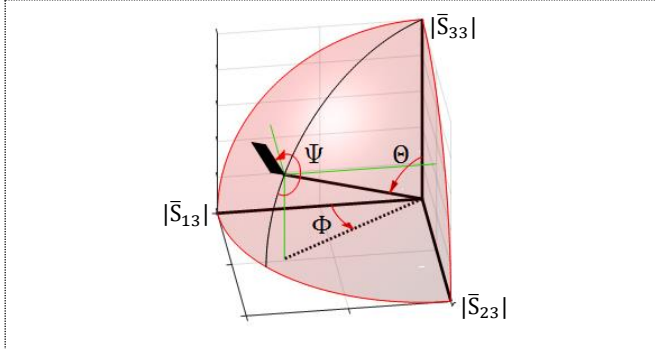
Figure 1: Geometric interpretation of the junction scattering parameters in terms of a spherical coordinate system. $\Theta = 62.55°$, $\Phi = 33.26°$, $\Psi = 246.02°$.
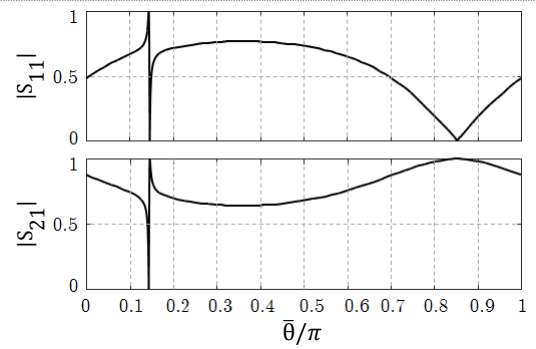

Figure 2: Example of a dual-mode resonator response: magnitude of the reflection (top) and transmission (bottom) coefficients, for the parameters of Fig. 1.

3. Example: high-contrast grating resonator

The model has been applied to the characterization of a high-contrast grating resonator. To this aim, Fig. 3 shows the HCG resonator response obtained with the RCWA, where the superimposed curves (resonance curves, where the half round trip phase shift is $n\pi$) indicate the presence of a resonance, and the color its Q factor (blue low, red high). Figure 4 shows the loci of the transmission (green) and reflection (red) zeros, and the resonance curves, obtained with our model in the neighborhood of the point P indicated in Fig. 3.
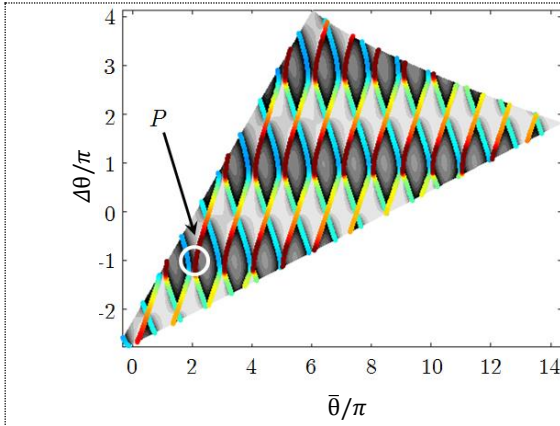

Figure 3: TE Reflectivity map for normal-incident plane wave (gray scale: brighter regions indicate high reflectivity). Abscissas and ordinates report the average and differential cavity electric lengths.
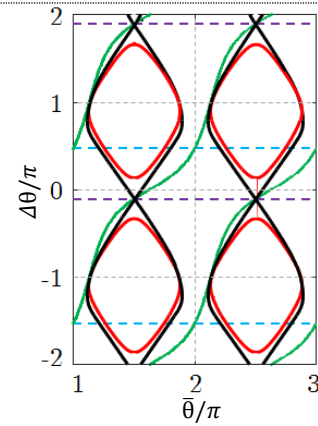

Figure 4: Curves representing the loci of the transmission (green) and reflection (red) zeros, and the resonance curves (black).

The analytic nature of our model allows to obtain simple closed-form expressions useful to understand several phenomena, such as the presence of high-Q Fano resonances (related to the tangency of the reflection and transmission zero loci), the 100% reflectivity at the crossing points between different resonance curves, or the existence of anticrossing regions [1].

Future works will deal with the ultrabroadband reflectivity features of HCGs.

4. References

[1]   C. J. Chang-Hasnain and W. Yang, "High-contrast gratings for integrated optoelectronics," *Adv. Opt. Photon.*, vol. 4, pp. 379-440, 2012.

[2]   M. G. Moharam and T. K. Gaylord, "Rigorous coupled-wave analysis of planar-grating diffraction," *J. Opt. Soc. Am.*, vol. 71, no. 7, pp. 811-818, July 1981.

[3]   A. Tibaldi, P. Debernardi, and R. Orta, "High-contrast gratings performance issues in tunable VCSELs," *IEEE J. Quantum Electron.*, vol. 51, no. 12, Dec. 2015.

[4]   R. Orta, A. Tibaldi, and P. Debernardi "Bimodal resonance phenomena," Part I, Part II, submitted to *IEEE J. Quantum Electron.*, July 2016.